RESEARCH   **Open Access**

The Role of Diffusion Weighted Imaging in suspected cases of ovarian cancer

Rahma Farghaly Ali[1*], Hana Hamdy Nassef[1], Ahmed Mohamed Ibrahim[2], Nivine Abdel Moneim Chalabi[1] and Asmaa Magdy Mohamed[1]

Abstract

Background: Ovarian cancer is a common gynecological malignancy and often diagnosed late with extensive peritoneal and nodal metastasis. Diffusion-weighted imaging (DWI) provides valuable information about the structural properties of the tissue and has shown great value in cancer imaging. Recently developed post-processing three-dimensional apparent diffusion coefficient (3D ADC) map has a significant value in variable tumors yet its role in ovarian cancer is not well established. We aim to evaluate the added value of DWI and 3D ADC maps in the diagnosis of ovarian masses, detection of nodal and peritoneal deposits, and so appropriate management planning.

Results: Conventional MRI and DWI were performed to fifty-one patients with complex cystic or solid adnexal lesions depicted by gynecological ultrasonography. Results were compared with surgical and histopathologic findings revealing 23/51 (45%) had malignant ovarian tumors and 28/51 (55%) had benign ovarian pathologies. The mean 3D ADC values were 0.977 ± 0.32, 0.934 ± 0.27, and $0.956 \pm 0.25 \times 10^{-3}$ mm^2/s for ovarian, nodal, and peritoneal malignancy respectively which were significantly lower than the mean 3D ADC values of benign ovarian lesions, non-metastatic lymph nodes and benign peritoneal lesions/fat which were measured 1.516 ± 0.6, 1.208 ± 0.25, and $1.46 \pm 0.43 \times 10^{-3}$ mm^2/s respectively.

Conclusion: Adding DWI and 3D ADC maps to routine MRI improves the sensitivity, specificity, and accuracy for detecting ovarian malignancy, nodal, and peritoneal metastasis. They also provide qualitative data helping in the differentiation of malignant and non-malignant entities.

Keywords: Conventional MRI, DWI, 3D ADC map, Ovarian malignancy, Peritoneal carcinomatosis

Background

Of all gynecological malignancy ovarian cancer represents about 2.5% and representing about 5% of female cancer death [1]. Primary ovarian tumors are divided into epithelial-stromal tumors, sex cord-stromal tumors, and germ cell tumors [2].

Malignant epithelial tumors account for 90% of all ovarian malignancy and include high grade serous ovarian cancer, low grade serous ovarian cancer, endometrioid carcinoma, clear cell carcinoma, and mucinous carcinoma [3]. Up to 65% of patients with epithelial carcinoma are diagnosed at FIGO stages III and IV with peritoneal and nodal deposits [4].

Secondary ovarian tumors mostly originate from the endometrium, the pancreas, the gastrointestinal tract, and the breast. Most of them are clinically and pathologically mimic the primary tumors [5].

Although staging laparotomy and histopathological examination are the gold standard methods for staging in all women suspected of having ovarian carcinoma, it is necessary to explore less invasive preoperative methods for staging and detection of nodal and peritoneal deposits [6].

The major roles of diagnostic imaging have been to characterize the ovarian mass, determine the extent of

* Correspondence: rahmafarghaly91@gmail.com
[1]Radiology Department, Faculty of Medicine, Ain Shams University, Cairo, Egypt
Full list of author information is available at the end of the article

preoperative disease, predict tumor resectability, and evaluate response to chemotherapy [7].

Pelvic and abdominal CT with both oral and intravenous (IV) contrast is the modality of choice in the pre-operative assessment of disease extension as well as predicting the success of surgical cytoreduction [8].

The doses of ionizing radiation to which the population has been exposed are increasingly higher due to its use in medical applications for the diagnosis and treatment of diseases. In 2008, the CT scan in the USA was the diagnostic technique that showed the highest dose deposition in the population [9]. So we are in need to use imaging techniques with low or no radiation hazards.

Ovarian cancer as other malignant tumors is characterized by neovascularization which predicts the metastatic properties of the tumor. Newly developed radiolabeled monoclonal antibodies have been settled for both the diagnosis and treatment of tumors in targeted radiotherapy [10].

MRI has flexibility for imaging anatomy, physiological parameters, and biochemical function, through appropriate choice of pulse sequences [11].

Diffusion MRI measures the diffusivity of endogenous water molecules in a tissue that reflects the mean size of the tissue microstructure that restricts and/or hinders the Brownian random motion of water molecules [12].

DWI allows the construction of 3D ADC maps of water molecules, that are promising markers of internal tumor pores and cellular gaps in which water molecules can migrate [11].

The primary focus of the research was the assessment of DWI for the qualitative evaluation of certain tumors. This focus has gradually shifted toward more quantitative methods of DWI assessment, including a large number of studies on the use of the main quantitative measure of DWI (ADC maps) [13].

Few articles have been reported; the diagnostic application of the DWI and ADC maps in the characterization and staging of ovarian tumors yet most of these studies have used the 2D ADC maps [14, 15].

This study evaluated the usefulness of diagnosis and preoperative staging of ovarian cancer (including characterization of ovarian lesions, detection of nodal, and peritoneal metastasis), using qualitative and quantitative analysis of DWI, and recently developed post-processing method (3D ADC maps).

Methods
Patients
This prospective study was performed from June 2018 till January 2020, and it included fifty-one adult females who had a complex cystic or solid adnexal lesion by trans-vaginal or trans-abdominal ultrasound examination with a mean age 45 ± 13.9-year-old (range of 16-74). Patients were referred to our radiology department in El-Demerdash Hospital for further assessment of the adnexal lesions.

Non-contrast MRI studies including conventional pelvic-abdominal images and DWI were done for all participants, after written consent was taken, according to the rules of our ethical committee. The results were confirmed by histopathology (Fig. 1).

The proper exclusion criteria were the following:

- Patients with previous adnexal surgical intervention
- Patients who received RTH or CTH or any treatment before MRI examination
- Patient with contraindication to MRI e.g. non-MRI compatible pacemaker

MRI examination

- Patients were injected with Buscopan intramuscularly 20 min before the examination to suppress bowel contractions, thereby avoiding DWI misreading of intestinal serosal deposits.
- MRI examination including conventional and DW images was done for all participants using 1.5 T Philips Achieva MRI unit with body Torso coil. The following conventional images were included:
- Pelvis MRI included
- Axial T1w-TSE (TR/TE, 550/24 ms), slice thickness 5 mm, gap 1 mm, and FOV 36 cm. Matrix 576 × 576.
- Axial T2w-TSE (TR/TE, 7649/115 ms), slice thickness 5 mm, gap 1 mm, and FOV 36 cm. Matrix 560 × 560.
- Sagittal and coronal T2-weighted, slice thickness 8-10 mm, gap 1 mm, and FOV 72-80 cm.
- DW-MRI was acquired in the axial plane by using a single-shot echo-planar imaging sequence with b values 0, 200, and 800, TR/TE 4274/63, slice thickness 5 mm, gap 1 mm, FOV 36 cm. Matrix 384 × 384.
- Abdomen MRI included
- Axial T2w-TSE (TR/TE, 450/80 ms), slice thickness 6 mm, gap 1 mm, and FOV 36 cm. Matrix 480 × 480.
- DW-3b (TR/TE 3793/65 ms), Slice thickness 6 mm, gap 1 mm, FOV 36 cm. Matrix 288 × 288.
- DWI at b value 800 was processed into inverted grayscale DWI using synapse. The SYNAPSE, Product Release Specification, Software Version 4.4, ENG-0034171-A, March 13th, 2015, SYNAPSE is a registered trademark of FUJIFILM Medical Systems, USA.
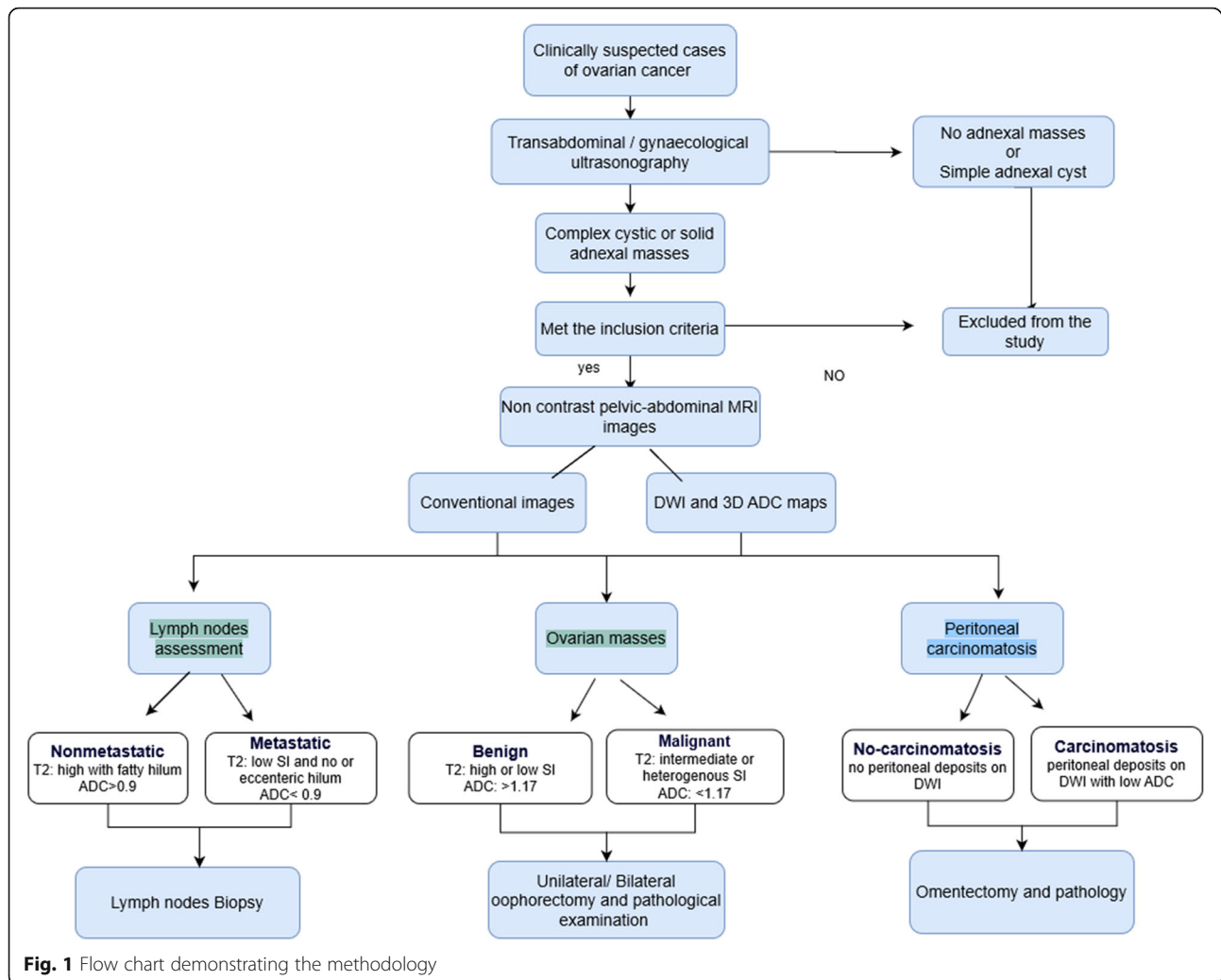
Fig. 1 Flow chart demonstrating the methodology

- 3D apparent diffusion coefficient (ADC) map was generated on the 3D synapse.
- The mean ADC values measured for the solid component of the ovarian lesions, lymph nodes, and peritoneal deposits.

Analysis of data

- The images were then reviewed by two gynecological radiologists (with 10 and 5 years' experience in female radiology) with specific points to comment on qualitative, and quantitative analysis of ovarian lesions, lymph nodes, and peritoneal carcinomatosis:
- Ovarian masses—unilateral or bilateral, solid or complex cystic (with septations, papillary projection, or soft tissue component), restricted or facilitated diffusion, and 3D ADC value of the solid component.

- Nodal assessment—site, size, restriction pattern compared to the solid component of ovarian masses, and 3D ADC value.
- Peritoneal thickening—presence or absence, size of nodules, anatomical site including omentum, peritoneal surface and serosa, and 3D ADC values.
- The two radiologists viewed the DWI and MRI data via a 3D synapse system without any knowledge of the pathological information. When there was a difference between them, a final decision was made by consensus.
- Forty-five patients underwent a total abdominal hysterectomy, oophorectomy, omentectomy, and lymph nodes biopsy. Six cases underwent unilateral oophorectomy. All results were correlated to the final post-operative histopathological data.

Statistical analysis

The data analysis was performed using the IBM SPSS statistics (V. 25.0, IBM Corp., USA, 2017-2018). For

quantitative parametric measurements, the data were expressed as mean ± SD. A receiver operating characteristic (ROC) curve was performed to assess the diagnostic accuracy of the measured ADC value for diagnosing malignant ovarian and nodal lesions using diagnostic validity tests which included sensitivity and specificity. *P* value < 0.05 was considered a statistically significant value. *P* value < 0.001 was considered a highly statistically significant value.

Results

This study included fifty-one female patients, their ages ranged between 16 and 74 years with mean age 45 ± 13.9 years old.

Characterization of ovarian lesions

From fifty-one cases, twenty-three cases showed malignant histopathology (45%) (Fig. 2) and twenty-eight cases showed benign histopathology (55%) (Table 1). Four cases showed bilateral ovarian lesions yet the most suspicious lesion of both ovarian lesions only included in this study to avoid bias.

The conventional MR combined with DW images were accurate in detecting ovarian malignancy yet 8 false-positive cases with solid components, intermediate or heterogeneous T2wi SI and low ADC values were reported, these cases were cases of necrotizing caseating granuloma, tubo-ovarian abscesses, mature cystic teratomas, infarcted ovary, and cystadenofibroma (Table 2).

These combined images showed 100% sensitivity, 71.4% specificity, 100% NPV, 74.2% PPV, and 84.3 % efficacy. Yet the accuracy of conventional MRI alone without DWI in the characterization of the ovarian lesion was 80% with 91.3% sensitivity, 64.29% specificity, 90% NPV, and 67.7% PPV.

In this study, two false-negative cases were reported, which were detected by the combined MRI/DWI yet were missed on conventional MRI alone, the first one was a very small malignant epithelial tumor, and the second one was ovarian surface small deposits secondary to malignant mesothelioma. Both of these malignant lesions were missed by conventional MRI images, yet restricted in the DWI.

Regarding ovarian lesions signal intensity in both DWI and 3D ADC map, 21/23 of malignant pathologies (91.3%) were restricted and only 2/23 pathologies (8.7%) were facilitated. The facilitated pathologies were metastatic from the colon with complex cystic morphology. Yet 17/28 benign lesions were restricted (60.7%) and 11/28 pathologies (39.3%) were facilitated. The restricted benign cases were cases of mature cystic teratomas, tubo-ovarian abscess, fibromas, fibrothecomas, cystadenofibroma, tubo-ovarian abscesses, and infarcted ovary.

The mean value of ADC of the malignant ovarian lesions was statistically significantly lower than that of the benign ovarian lesions (0.977 ± 0.3 and 1.516 ± 0.6 respectively) (Table 3).

Based on the area under the ROC curve of 0.756, the cutoff value below which malignancy is expected is less than 1.17×10^{-3} mm^2/s with 69.9% sensitivity, and 75% specificity (Fig. 3).

Detection of nodal deposits

The histopathological results assessed only in forty-seven patients out of the fifty-one patients, and it revealed metastatic LN in eleven cases, yet the LN was benign in thirty-six cases.

The conventional MR combined with DW images were accurate in detecting metastatic LNs yet 5 false-positive cases with low ADC values were reported, three of them were associated with benign ovarian pathologies (necrotizing caseating granuloma and tubo-ovarian abscesses) and two associated with malignant ovarian
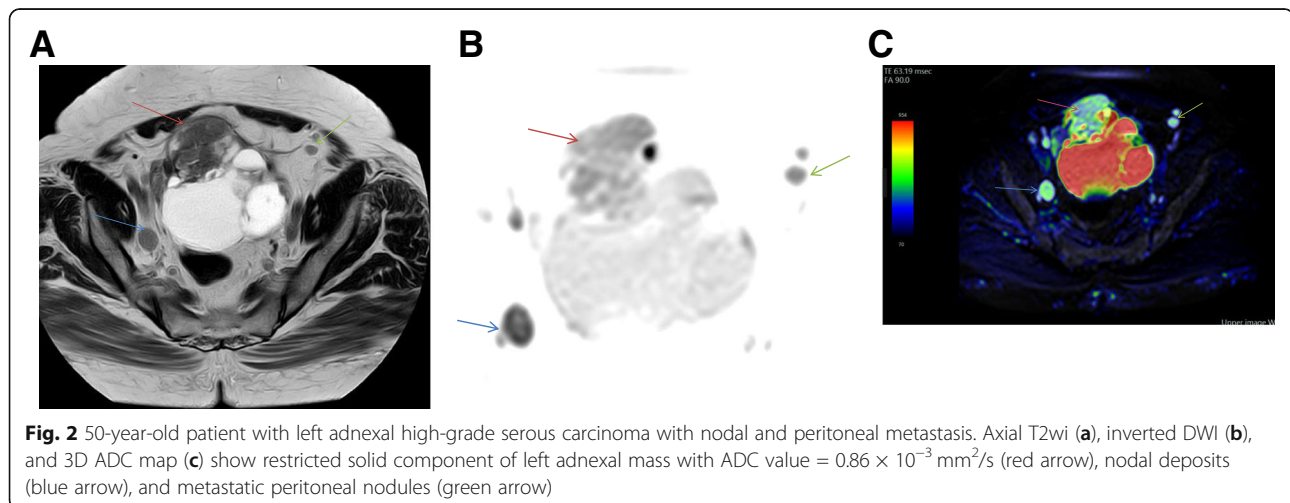

Fig. 2 50-year-old patient with left adnexal high-grade serous carcinoma with nodal and peritoneal metastasis. Axial T2wi (**a**), inverted DWI (**b**), and 3D ADC map (**c**) show restricted solid component of left adnexal mass with ADC value = 0.86×10^{-3} mm^2/s (red arrow), nodal deposits (blue arrow), and metastatic peritoneal nodules (green arrow)

Table 1 Ovarian masses pathological classification

Ovarian lesions subtypes			
Malignant	NB (%)	Benign	NB (%)
*Primary ovarian tumors		Serous cystadenoma	7 (13.7%)
High-grad papillary serous	6 (11.7)	Mature teratoma	3 (5.9%)
Low-grade papillary serous	4 (7.8%	Mucinous cystadenoma	3 (5.9%)
Mucinous adenocarcinoma	1 (1.9%)	Fibrothecoma	3 (5.9%)
Endometrioid adenocarcinoma	1 (1.9%)	Fibroma	2 (3.9%)
Malignant germ cell tumor	2 (3.9%)	Endometrioid cystadenoma	1 (1.9%)
Malignant granulosa cell	1 (1.9 %)	Endometrioidcystadenofibroma	1 (1.9%)
Malignant endodermal sinus tumor	1 (1.9%)	Endometriosis with abscess	2 (3.9%)
*Metastatic ovarian tumors		Tubo-ovarian abscess	4 (7.8%)
Endometrial cancer	2 (3.9%)	Necrotizing caseating granuloma	1 (1.9%)
Uterine leiomyosarcoma	1 (1.9%)	Infarcted ovary	1 (1.9%)
Colon adenocarcinoma	2 (3.9%)		
Gastric carcinoma	1 (1.9%)		
Malignant mesothelioma	1 (1.9%)		

pathologies with histopathologically proven free lymph nodes (Table 2).

The combined images showed 100% sensitivity, 86.1% specificity, 100% NPV, 68.8% PPV, and 89.4% efficacy in detecting LNs deposits. Yet the accuracy of conventional MRI alone without DWI was 76.6% with 63.64% sensitivity, 80.56% specificity, 87.88% NPV, and 50% PPV.

Conventional MRI images showed lower sensitivity than that of combined images in the detection of nodal metastasis as 4/11(36.37%) of metastatic lymph nodes were small and missed by conventional images.

The mean 3D ADC value of malignant nodal deposits was statistically significantly lower than that of the non-metastatic lymph nodes (measured 0.934 ± 0.27 and 1.208 ± 0.25 respectively) (Table 3).

The lymph node restriction degree compared to that of the solid component of the ovarian masses was statistically significant in differentiating metastatic and non-metastatic lymph nodes with $p = 0.000$ (Table 4). As 45.5% of metastatic lymph nodes had the same degree of restriction compared to the solid component of ovarian masses and 36.4% were restricted more than the solid component. This compared to 8.3% of the non-metastatic lymph nodes which had the same degree of restriction as to the solid component and 2% of them were restricted more than the solid component of ovarian masses.

Based on the area under the ROC curve of 0.868 the cutoff value below which malignancy is expected is less than $0.9 \times 10^{-3}\,mm^2/s$ with 63.6% sensitivity, and 80.6% specificity (Fig. 3).

Table 2 Conventional MRI combined with DWI in detection of ovarian malignancy, nodal, and peritoneal deposits correlated to histopathology

Conventional MRI and DWI		Histopathology		Pearson chi-square	
		Malignant	Non-malignant	Value	P*
Ovarian Masses	Malignant	23 (100%)	8 (28.6%)	27.028[a]	0.000
	Benign	0 (0%)	20 (71.4%)		
	Total	23 (100%)	28 (100%)		
Lymph nodes	Metastatic	11 (100%)	5 (13.9%)	27.825[a]	0.000
	Non-metastatic	0 (0%)	31 (86.1%)		
	Total	11 (100%)	36 (100%)		
Peritoneal deposits	Carcinomatosis	18 (100%)	3 (9%)	39.7403[a]	0.000
	No carcinomatosis	0 (0%)	30 (90.9%)		
	Total	18 (100%)	33 (100%)		

Chi-square tests—P value > 0.05, non significant; P value < 0.05, significant; P value < 0.001, highly significant
[a]the significance level

Table 3 Mean 3D ADC values of histopathologically proved malignant and non-malignant ovarian lesions, lymph nodes, and peritoneal deposits

	Pathology	N	Mean value	P*
Ovarian masses	Benign	28	1.516 ± 0.6	0.003
	Malignant	23	0.977 ± 0.3	
Lymph nodes	Non-malignant	36	1.208 ± 0.25	0.006
	Malignant	11	0.934 ± 0.27	
Peritoneal deposits	No carcinomatosis	33	1.46 ± 0.43	0.001
	Carcinomatosis	18	0.956 ± 0.25	

Wilcoxon rank-sum test—ADC value ($\times 10^{-3}$ mm^2/s)

*P value > 0.05, non significant; P value < 0.05, significant; P value < 0.01, highly significant

Assessment of peritoneal deposits

Peritoneal carcinomatosis was histopathologically confirmed in 18 cases (35.3%) (Fig. 4), other thirty-three cases (64.7%) had no carcinomatosis with only three cases showing benign peritoneal thickening on histopathology (Figs. 5 and 6).

The combined conventional MR and DW images were accurate in detecting peritoneal carcinomatosis (Table 2) with 100% sensitivity, 90.91% specificity, 100% NPV, 85.71% PPV, and 94.12% efficacy.

Yet the accuracy of conventional MRI alone without DWI in the detection of peritoneal deposits was 90.2% with 88.89% sensitivity, 90.91% specificity, 93.75% NPV, and 84.21% PPV.

Three false-positive cases associated with benign ovarian pathologies two of them were diffuse granulomatous and inflammatory thickening in cases of necrotizing caseating granuloma, tubo-ovarian abscess. The third one showed small nodular thickening (peritoneal particulates) which was seen in the case of ovarian infarction.

Two false-negative cases in the form of tiny peritoneal metastatic deposits were missed by conventional MRI alone and detected by DWI.

Peritoneal carcinomatosis deposits were smaller than 10 mm in two cases (11.1%) and larger than 10 mm in five cases (27.8), yet it was confluent in eleven cases (61.1%). Non-malignant peritoneal thickening was smaller than 10 mm in one case (3%) and confluent in two cases (6.1%) (Table 5).

The mean 3D ADC value of peritoneal carcinomatosis was statistically significantly lower than that of non-carcinomatosis (including the ADC value of peritoneal fat in cases where there were no peritoneal thickening and the ADC value of benign peritoneal thickening) measuring 0.956 ± 0.25 and 1.46 ± 0.43 respectively (Table 3).

Discussion

Ovarian cancer is often diagnosed late with extensive peritoneal metastases [FIGO stages IIIc and IV], decreasing the patient's survival rate to 10 % in FIGO stage IV and 20–40 % in FIGO stage IIIc disease [16] (Fig. 3).

Cancer staging is a fundamental principle and one of the first and most important steps used to predict the patient outcomes as well as to plan the most appropriate treatment [17].

In this study, DWI combined with conventional MR images were used for staging of ovarian cancer aiming that these non-contrast MRI images may become the exam of choice in patients with absolute or relative contraindications to contrast media, e.g., pregnant females (this study included two pregnant cases).
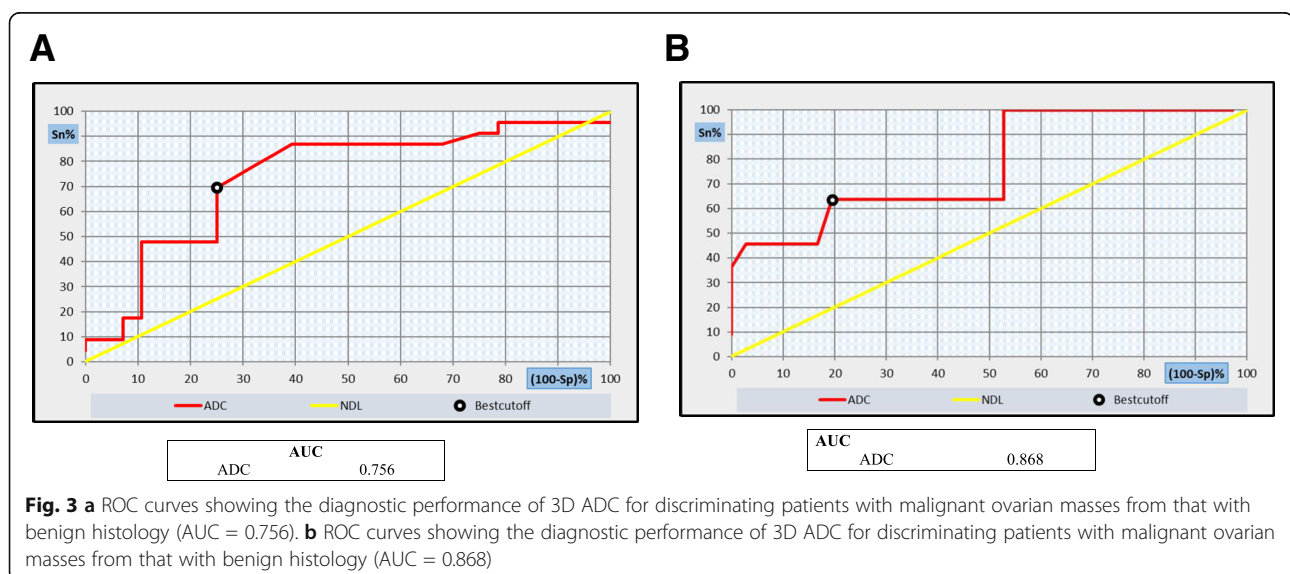

Fig. 3 a ROC curves showing the diagnostic performance of 3D ADC for discriminating patients with malignant ovarian masses from that with benign histology (AUC = 0.756). **b** ROC curves showing the diagnostic performance of 3D ADC for discriminating patients with malignant ovarian masses from that with benign histology (AUC = 0.868)

Table 4 Degree of lymph nodes restriction compared to the solid component of ovarian masses

		Histopathogy	
		Benign	Malignant
Nodal/ solid component restriction	< Solid component	31 (86.1%)	2 (18.2%)
	= Solid component	3 (8.3%)	5 (45.5%)
	> Solid component	2 (5.6%)	4 (36.4%)
	Value	P*	
Pearson chi-square	19.434[a]	0.000	

Chi-square test
*P value > 0.05, non significant; P value < 0.05, significant; P value < 0.01: Highly significant

To our knowledge, this was the first study that used a 3D ADC map in preoperative staging of ovarian cancer. This study included quantitative and qualitative analysis of ovarian masses, lymphatic metastasis, and peritoneal deposits. Yet other studies used 2D ADC maps in the staging of ovarian malignancy.

In this study, combined DW and conventional MRI images showed a high sensitivity (100%) for the detection of ovarian pathology yet low specificity (71.4%). This low specificity could be explained by the presence of eight false-positive cases (eight benign adnexal masses that mimicked malignancy). All these cases showed solid adnexal lesions components displayed intermediate or heterogeneous T2wi SI and low ADC values. These cases included necrotizing caseating granuloma, tubo-ovarian abscesses, mature cystic teratomas, infarcted ovary, and cystadenofibroma with mean 3D ADC values of $1.3 \times 10^{-3}\,\mathrm{mm^2/s}$, $0.63 \times 10^{-3}\,\mathrm{mm^2/s}$, $0.9 \times 10^{-3}\,\mathrm{mm^2/s}$, $0.53 \times 10^{-3}\,\mathrm{mm^2/s}$, and $1.2 \times 10^{-3}\,\mathrm{mm^2/s}$ respectively. Few cases of them were also associated with benign peritoneal thickening and enlarged lymph nodes with low 3D ADC values as in cases of necrotizing caseating granuloma and case of tubo-ovarian abscess.
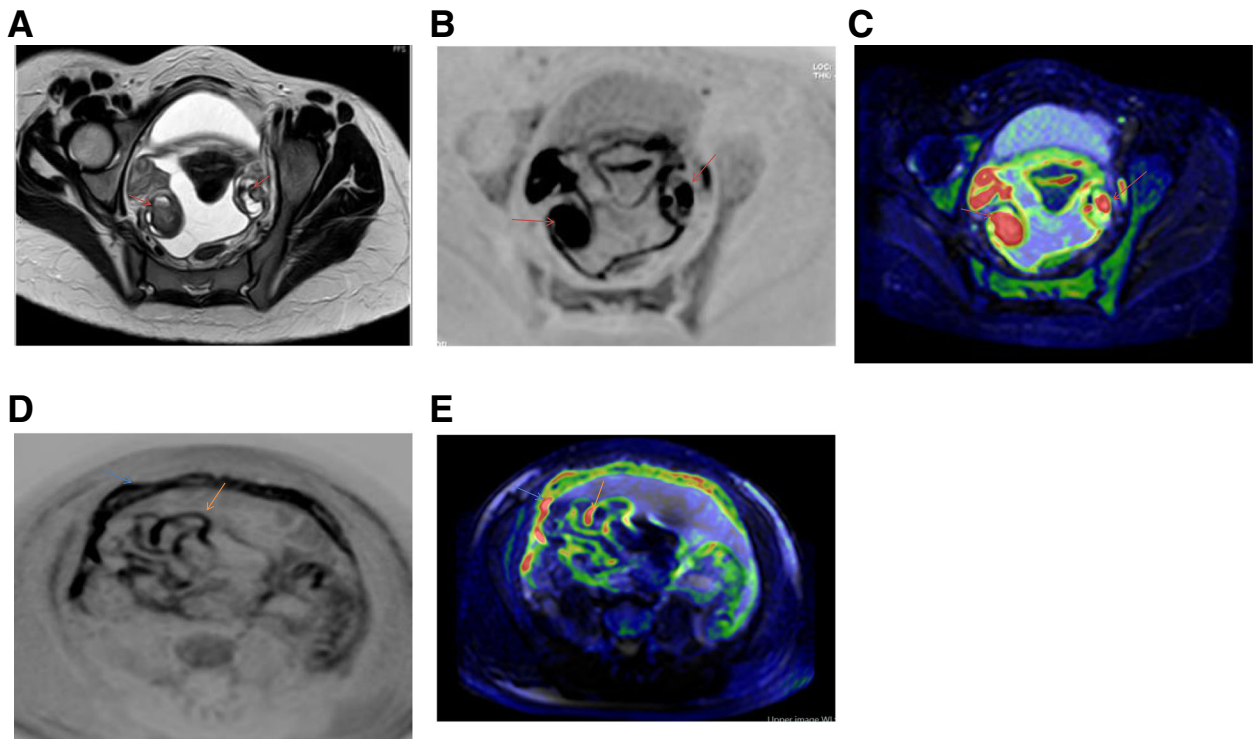

Fig. 4 a Inverted DWI and 3D ADC map showing hepatic surface deposits in case of malignant endodermal sinus tumor (**a** and **b**). **b** Diffuse peritoneal deposits in a case of metastatic leiomyosarcoma as demonstrated by red arrows in inverted DWI and 3D ADC map (**c** and **d**)
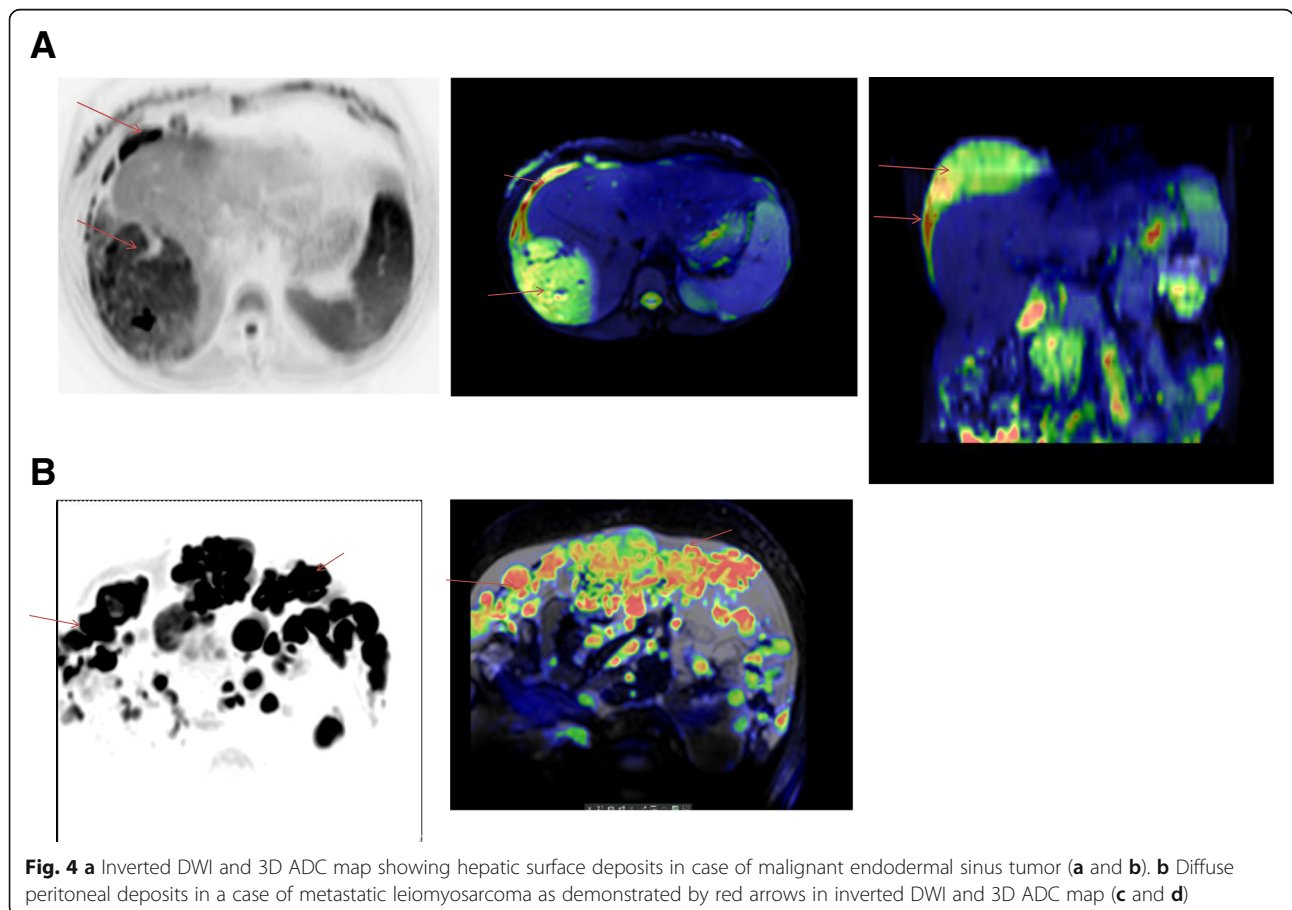
Fig. 5 23-year-old female with bilateral adnexal necrotizing caseating granuloma (**b**) associated with peritoneal and hepatic involvement. Bilateral complex adnexal cystic lesions are seen in axial T2WI of the pelvis (**a**). Solid components showing restricted diffusion (red arrows) in both inverted DWI and 3D ADC maps (**b** and **c**). Inverted DWI and 3D ADC map of the pelvis (**d** and **e**) showing diffuse peritoneal surface (blue arrows) and bowel serosal thickening (orange arrows)

In this study, the mean 3D ADC values for benign ovarian lesions were $1.516 \pm 0.6 \times 10^{-3}$ mm^2/s and for malignant lesions were $0.977 \pm 0.3 \times 10^{-3}$ mm^2/s and the cutoff value below which malignancy is expected is less than 1.17×10^{-3} mm^2/s with 69.9% sensitivity, 75% specificity, 75% NPV, and 69.6% PPV.

Takeuchi et al. [18], in their study which included 49 ovarian tumors, 39 of them were malignant/borderline malignant and 10 were benign tumors, found that the mean 2 D ADC value for malignant tumors was significantly lower than that in benign tumors (measured 1.03 ± 0.19 and 1.38 ± 0.30 respectively). They also
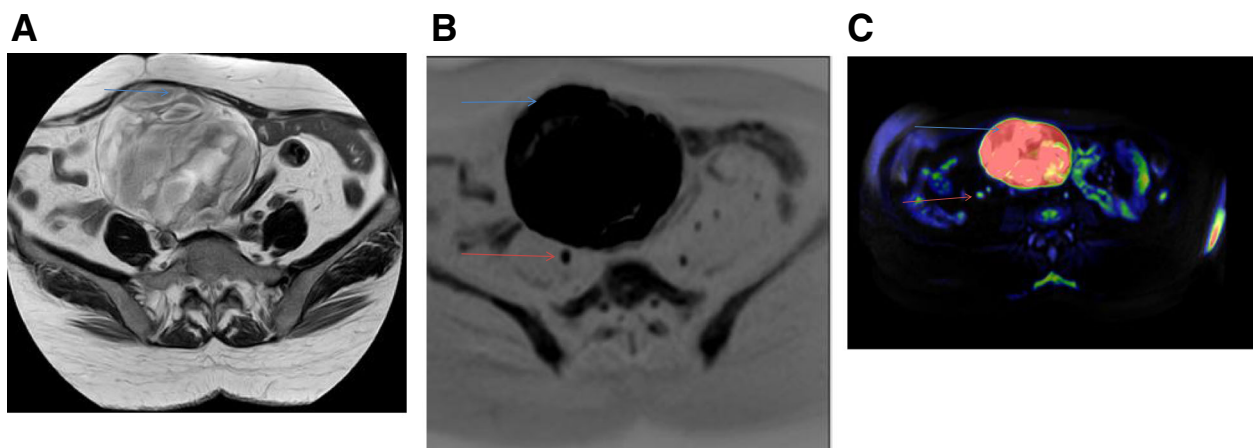
Fig. 6 58-year-old patient with right ovarian infarction and peritoneal particulates. A right complex adnexal lesion with heterogeneous SI in T2wi as seen in figure **a**. Lesion is truly restricted (blue arrows) with ADC value = 0.53×10^{-3} mm^2/s as seen in inverted DWI and 3D ADC map (**b** and **c**). Small peritoneal lesions also noted (green arrow)

Table 5 The size of peritoneal thickening/ deposits correlated to histopathology

		Histopathology		
		No carcinomatosis	Carcinomatosis	Total
Size of peritoneal nodules by MRI	No nodules	30 (90.9%)	0 (0%)	30 (58.8%)
	nodules < 10 mm	1 (3%)	2 (11.1%)	1 (2%)
	nodules > 10 mm	0 (0%)	5 (27.8%)	5 (9.8%)
	Confluent	2 (6.1%)	11 (61.1%)	15 (29.4%)
Total		33 (100%)	18 (100%)	51 (100%)

found the cutoff ADC value of 1.15 malignant lesions had 74% sensitivity, 80% specificity, 94% PPV, and 44% NPV. The mean ADC value for malignancy was higher than that of this study as this study included malignant ovarian lesions with low ADC values as leiomyosarcoma, and uterine adenocarcinoma with metastatic deposits to ovaries with ADC values 0.4, and 0.6 respectively such cases not included in their study.

Li et al. [19], in their study which included 127 patients with 131 lesions, 46 of them were benign and 81 were malignant, found that the 2D mean ADC value for benign lesions was 1.69×10^{-3} mm^2/s $\pm$ 0.25 SD, and $1.03 \times 10^{-3} \pm 0.22$ SD mm^2/s for malignant lesions. The cut off value was 1.25×10^{-3} mm^2/s showed 90.1% sensitivity and 89.9% specificity. A lower mean ADC value of benign ovarian masses in this study may attribute to the presence of non-malignant ovarian lesions with low ADC value as tubo-ovarian abscess, infarcted ovary, and necrotizing caseating granuloma, such cases not included in their study as their study only included ovarian lesions originated from surface epithelium.

This is in contrary to the results of El Ameen et al. [20] who had a lower cut off value, and mean ADC value for malignancy (1×10^{-3} mm^2/s, and 0.8×10^{-3} mm^2/s $\pm$ 0.1 SD respectively). This may attribute to the presence of metastatic cystic tumors from colon included in this study with high ADC values of 1.7×10^{-3} mm^2/s and 1.9×10^{-3} mm^2/s. These cases of metastatic adnexal tumors from the colon presented with complex cystic ovarian lesions and by MRI colonic masse were detected with multiple air-fluid levels in one of them. Yet they agreed with this study regarding the sensitivity, specificity, NPV, PPV, and accuracy of conventional MRI without DWI in the characterization of ovarian lesions (92%, 61.11%, 84.6%, 76.7%, and 79.1%).

Previous studies have suggested that quantitative 2 D ADC analysis may be useful for staging of ovarian cancers and predicting responses to chemotherapy [21–23].

To our knowledge, few studies exploring relationships between ADC values of lymph nodes and lymphatic metastasis were done, one of them performed by Wang et al. [24], including 49 patients with 29 negative cases (59.2%) and 20 positives (40.8%). They agreed with us regarding the statistical significance of ADC values in

the detection of metastatic nodal deposits with $p = 0.000$. Yet their study showed a higher cut off value (1.003×10^{-3} mm^2/s) with higher specificity (93.1%). Such lower specificity in this study can be attributed to the presence of acute lymphadenitis in cases of necrotizing caseating granuloma and tubo-ovarian abscess showed low ADC values and reported as malignant lymph nodes.

Other studies also concluded the accuracy of DWI in the characterization of ovarian masses and detection of nodal deposits [8, 19, 21].

In this study, the conventional MR combined with DW images were accurate in detecting peritoneal carcinomatosis with 100% sensitivity, 90.91% specificity, 100% NPV, 85.71% PPV, and 94.12% efficacy. The size of peritoneal carcinomatosis was smaller than 1 cm in 11.1 % and larger than 1 cm in 27.8% and 61.1 % showed confluent disease.

Michielsen et al. [14] found that DWI/MRI was accurate in detecting peritoneal carcinomatosis with 91% sensitivity, 91% specificity, 89% PPV, 93% NPV, and 91% accuracy. The size of peritoneal carcinomatosis in their study was smaller than 1 cm in 36% and larger than 1 cm in 29% and 35% showed confluent disease. Higher sensitivity in this study may be attributed to a greater percentage of cases with confluent peritoneal disease and may be also attributed to the sensitivity of 3D ADC colored maps.

Other studies also showed the accuracy of DWI in the detection of peritoneal carcinomatosis (qualitative analysis) [25–28]. Yet few studies concerned with quantitative analysis of peritoneal carcinomatosis.

In this study, the mean 3D ADC value of peritoneal carcinomatosis at b value 800 was $0.956 \pm 0.25 \times 10^{-3}$ mm^2/s. Onur et al. [29], in their study which included 28 oncology patients six of them had ovarian cancer, found that the mean ADC value at b value 1000 was 1.09 ± 0.4 ($\times 10^{-3}$ mm^2/s). A lower mean ADC value for peritoneal carcinomatosis in this study may be attributed to low ADC value peritoneal deposits as in cases of metastatic leiomyosarcoma and peritoneal mesothelioma.

In this study, the mean ADC value of both peritoneal carcinomatosis and malignant lymphadenopathy is

slightly lower than that of ovarian cancer. In certain cases as cases of tubo-ovarian abscesses, necrotizing caseating granuloma, and ovarian infarction especially in elderly patients, ovarian lesions were mimic of that ovarian cancer as they had low ADC values, associated with peritoneal nodules, and enlarged lymphadenopathy, especially in first two cases so proper history and clinical data are very important for proper diagnosis and management.

In this study, the 3D ADC map was helping in proper assessment of ovarian masses, peritoneal, and nodal deposits. Few studies were done to evaluate the role of 3D ADC maps in discrimination of different tumor histological grading and other studies compared the role of 3D and 2D ADC maps.

Moryia and colleagues [30] used 3D ADC histogram in the differentiation of different histological types of hepatocellular carcinomas and they found that the minimum ADC was the most promising parameter for distinguishing poorly differentiated HCC from the other histological grades.

Tamada et al. [31], in their study which compared the reproducibility and diagnostic performance of 2D and 3D ROIs for prostatic ADC measurements, found that the use of 3D ROI did not improve the intrareader or inter-reader reproducibility or the diagnostic performance compared with the use of 2D ROI.

This was in contrary to the study done by Lui and colleagues [32] comparing the whole tumor 3D and 2D center-slice analysis in both ADC maps of b800 and b1000 and they suggested that the whole tumor 3D analysis of ADC maps provide reliable results and a more comprehensive evaluation of tumor histological grade.

Another study was done by Souza and colleagues [33] in which they compared mean ADC values calculated in 2D and 3D for differentiating healthy brain tissues, glioblastoma, and meningioma and they found that 2D and 3D ADC maps could possibly differentiate meningiomas and glioblastomas or glioblastomas from normal tissues. However, meningiomas and normal tissues can be confused in the 3D analysis because of different cellularity and cellular type variability.

This study had several limitations such as the unequal distribution of ovarian pathologies included in the study and the limited number of cases with primary ovarian malignancy. Our study depended on 3D ADC maps and 2D maps were not included. Furthermore, a limitation related to the cost, availability, and the contraindication of MRI examination was encountered.

A future comparative study comparing and evaluating the diagnostic performance of 2D and 3D ovarian ADC maps with a larger sample number and better pathological distribution is recommended.

Conclusion

Adding DWI and recently developed processed 3D ADC maps to the conventional MR images provides quantitative and qualitative analysis of the ovarian masses, lymph nodes, and peritoneal deposits and hence, increasing the sensitivity, specificity, and accuracy of the non-contrast conventional images. Therefore DWI, and recently developed post-processing 3D ADC, may become promising techniques with applications in various areas of ovarian cancer imaging including diagnosis, staging, and treatment planning especially in patients with relative or absolute contraindications to the use of contrast material.

Author details
[1]Radiology Department, Faculty of Medicine, Ain Shams University, Cairo, Egypt. [2]Obstetrics and Gynecology Department, Faculty of Medicine, Ain Shams University, Cairo, Egypt.

References
1. Torre LA, Trabert B, DeSantis CE et al (2018) Ovarian cancer statistics, 2018. CA Cancer J Clin 68:284–296. https://doi.org/10.3322/caac.21456
2. Javadi S, Ganeshan DM, Qayyum A et al (2016) Ovarian cancer, the revised FIGO staging system, and the role of imaging. Am J Roentgenol 206(6): 1351–1360 https://doi.org/10.2214/AJR.15.15199
3. Kiyokawa T, Iwamoto M (2018) Current concept of precancerous and early stage of serous ovarian carcinoma. In: Moriya T (ed) Pathology of Female Cancers. Springer, Singapore https://doi.org/10.1007/978-981-10-8606-9_4
4. Prado AG, Hernando CG, Delgado DV et al (2019) Diffusion-weighted magnetic resonance imaging in peritoneal carcinomatosis from suspected ovarian cancer: diagnostic performance in correlation with surgical findings. Eur J Radiol 121:108696 ISSN 0720-048X. https://doi.org/10.1016/j.ejrad.2019.108696

5.   Kehr E, Soong TR, Hirsch MS (2018) Chapter 28 - Metastatic tumours involving the ovary. In: Crum CP, Nucci MR, Howitt BE, Granter SR, Parast MM, Boyd TK (eds) Diagnostic Gynecologic and Obstetric Pathology (Third Edition), pp 1050–1069 ISBN 9780323447324. https://doi.org/10.1016/B978-0-323-44732-4.00028-5

6.   Pu T, Xiong L, Liu Q et al (2017) Delineation of retroperitoneal metastatic lymph nodes in ovarian cancer with near-infrared fluorescence imaging. Oncol Lett 14:2869–2877 https://doi.org/10.3892/ol.2017.6521

7.   Kang SK, Reinhold C, Atri M et al (2018) ACR Appropriateness Criteria ® staging and follow-up of ovarian cancer, expert panel on women's imaging. J Am Coll Radiol 15(5):S198–S207 https://doi.org/10.1016/j.jacr.2018.03.015

8.   Schmidt S, Meuli RA, Achtari C et al (2015) Peritoneal carcinomatosis in primary ovarian cancer staging: comparison between MDCT, MRI, and 18F-FDG PET/CT. Clin Nucl Med 40(5):371–377 https://doi.org/10.1097/RLU.0000000000000768

9.   Gómez AML, Santana PC, Mourão AP (2020) Dosimetry study in head and neck of anthropomorphic phantoms in computed tomography scans. Sci Med J 2(1):38–43 https://doi.org/10.28991/SciMedJ-2020-0201-6

10. Yavari K (2018) Anti-angiogenesis therapy of cancer cells using 153Sm-Bevasesomab. Emerg Sci J 2(3):130–139

11. Bonekamp S, Corona-Villalobos CP, Kamel IR (2012) Oncologic applications of diffusion weighted MRI in the body. J Magn Reson Imaging 35:257–279 https://doi.org/10.1002/jmri.22786

12. Kim S, Loevner L, Quon H et al (2009) Diffusion-weighted magnetic resonance imaging for predicting and detecting early response to chemoradiation therapy of squamous cell carcinomas of the head and neck. Clin Cancer Res 15(3):986–989 https://doi.org/10.1158/1078-0432.CCR-08-1287

13. Amodeo S, Rosman AS, Desiato V et al (2018) MRI-based apparent diffusion coefficient for predicting pathologic response of rectal cancer after neoadjuvant therapy: systematic review and meta-analysis. Am J Roentgenol 211(6):W 205–W 216

14. Michielsen K, Vergote I, Op de Beeck K et al (2014) Whole-body MRI with diffusion-weighted sequence for staging of patients with suspected ovarian cancer: a clinical feasibility study in comparison to CT and FDG-PET/CT. Eur Radiol 24:889–901 https://doi.org/10.1007/s00330-013-3083-8

15. Baboli M, Zhang J, Kim SG (2019) Advances in diffusion and perfusion MRI for quantitative cancer imaging. Curr Pathobiol Rep 7:129–141 https://doi.org/10.1007/s40139-019-00204-7

16. Ferlay J, Parkin DM, Steliarova-Foucher E (2010) Estimates of cancer incidence and mortality in Europe in 2008. Eur J Cancer 46:765–781 https://doi.org/10.1016/j.ejca.2009.12.014

17. Prat J, FIGO Committee on Gynecologic Oncology (2015) FIGO's staging classification for cancer of the ovary, fallopian tube, and peritoneum: abridged republication. J Gynecol Oncol 26(2):87–89 https://doi.org/10.3802/jgo.2015.26.2.87

18. Takeuchi M, Matsuzaki K, Nishitani H et al (2010) Diffusion-weighted magnetic resonance imaging of ovarian tumours: differentiation of benign and malignant solid components of ovarian masses. J Comput Assist Tomogr 34:173e6 https://doi.org/10.1097/RCT.0b013e3181c2f0a2

19. Li W, Chu C, Cui Y, et al. (2012) Diffusion-weighted MRI: a useful technique to discriminate benign versus malignant ovarian surface epithelial tumours with solid and cystic components. Abdom Radiol 37, 897–903. https://doi.org/10.1007/s00261-011-9814-x

20. El Ameen NF, Eissawy MG, Mohsen LAMS et al (2020) MR diffusion versus MR perfusion in patients with ovarian tumours; how far could we get? Egypt J Radiol Nucl Med 51:35 https://doi.org/10.1186/s43055-020-0141-5

21. Klerkx WM, Mali WM, Heintz AP et al (2011) Observer variation of magnetic resonance imaging and diffusion-weighted imaging in pelvic lymph node detection. Eur J Radiol 78(1):71–74. https://doi.org/10.1016/j.ejrad.2009.04.027

22. Li HM, Qiang JW, Xia GL et al (2015) MRI for differentiating ovarian endometrioid adenocarcinoma from high-grade serous adenocarcinoma. J Ovarian Res 8:26 https://doi.org/10.1186/s13048-015-0154-2

23. Oh JW, Rha SE, Oh SN et al (2015) Diffusion-weighted MRI of epithelial ovarian cancers: correlation of apparent diffusion coefficient values with histologic grade and surgical stage. Eur J Radiol 84(4):590–595 https://doi.org/10.1016/j.ejrad.2015.01.005

24. Wang F, Wang Y, Zhou Y et al (2017) Comparison between types I and II epithelial ovarian cancer using histogram analysis of monoexponential, biexponential, and stretched-exponential diffusion models. J Magn Reson Imaging 46:1797–1809. https://doi.org/10.1002/jmri.25722

25. Michielsen K, Dresen R, Vanslembrouck R et al (2017) Diagnostic value of whole-body diffusion-weighted MRI compared to computed tomography for pre-operative assessment of patients suspected for ovarian cancer. Eur J Cancer 83:88–98 https://doi.org/10.1016/j.ejca.2017.06.010

26. Vergote I, Van Gorp T, Amant F et al (2008) Timing of debulking surgery in advanced ovarian cancer. Int J Gynecol Cancer 18(Suppl 1):11–19. https://doi.org/10.1111/j.1525-1438.2007.01098.x

27. Espada M, Garcia-Flores JR, Jimenez M et al (2013) Diffusion-weighted magnetic resonance imaging evaluation of intraabdominal sites of implants to predict likelihood of suboptimal cytoreductive surgery in patients with ovarian carcinoma. Eur Radiol 23:2636–2642 https://doi.org/10.1007/s00330-013-2837-7

28. Low RN, Sebrechts CP, Barone RM et al (2009) Diffusion weighted MRI of peritoneal tumours: comparison with conventional MRI and surgical and histopathologic findings–a feasibility study. Am J Roentgenol 193(2):461–470. https://doi.org/10.2214/AJR.08.1753

29. Onur MR, Akyol M, Poyraz AK et al (2012) Diagnosis of peritoneal metastases with abdominal malignancies: role of ADC measurement on diffusion weighted MRI. Eurasian J Med 44(3):163–168 https://doi.org/10.5152/eajm.2012.38

30. Moriya T, Saito K, Tajima Y et al (2017) 3D analysis of apparent diffusion coefficient histograms in hepatocellular carcinoma: correlation with histological grade. Cancer Imaging 17:1 https://doi.org/10.1186/s40644-016-0103

31. Tamada T, Huang C, Ream JM et al (2018) Apparent diffusion coefficient values of prostate cancer: comparison of 2D and 3D ROIs. Am J Roentgenol 210(1):113–117 https://doi.org/10.2214/AJR.17.18495

32. Liu Y, Zhang Y, Cheng R et al (2019) Radiomics analysis of apparent diffusion coefficient in cervical cancer: a preliminary study on histological grade evaluation. J Magn Reson Imaging 49:280–290. https://doi.org/10.1002/jmri.26192

33. Souza M, Castellano G, Baldissin MM et al (2012) Comparison of ADC values obtained in 2D and 3D for differentiation between healthy brain tissues, glioblastoma and meningioma. World Congress on Medical Physics and Biomedical Engineering May 26-31, 2012, Beijing, pp 975–978 https://doi.org/10.1007/978-3-642-29305-4_256

Publisher's Note

Springer Nature remains neutral with regard to jurisdictional claims in published maps and institutional affiliations.